Centrum voor Wiskunde en Informatica
Centre for Mathematics and Computer Science

H.A. Lauwerier

Global bifurcation of a logistic delay map

Department of Applied Mathematics Report AM-R8402 January

Bibliotheek
Centrum voor Wiskunde en Informatica
Amsterdam

CWI BIBLIOTHEEK
3 0054 00095 5808

The Centre for Mathematics and Computer Science is a research institute of the Stichting Mathematisch Centrum, which was founded on February 11, 1946, as a nonprofit institution aiming at the promotion of mathematics, computer science, and their applications. It is sponsored by the Dutch Government through the Netherlands Organization for the Advancement of Pure Research (Z.W.O.).

Copyright © Stichting Mathematisch Centrum, Amsterdam

GLOBAL BIFURCATION OF A LOGISTIC DELAY MAP

H.A. LAUWERIER
Centre for Mathematics and Computer Science, Amsterdam

We consider the planar map $x' = y$, $y' = \phi(x,y)$ connected to the difference $x_{n+1} = ax_n(1-(1-b)x_n-bx_{n-1})$ with $a > 1$, $0 < b < 1$. The unstable manifold of the fixed point $(0,0)$ is determined explicitly as an analytic curve. The stable manifold consists of an infinity of algebraic curves and forms the boundary of the escape region, the set of starting-points of orbits going to infinity. The case $b = \frac{1}{2}$ is studied in more detail and most illustrations are for this case. For $a > 3$ there always exists an unstable 4-cycle. For this cycle the secondary unstable manifolds are also determined explicitly. Still for the case $b = \frac{1}{2}$ a Feigenbaum scenario of repeated period-doubling has been observed. However, the convergence to Feigenbaum's universal constant appears to be rather slow.

1980 MATHEMATICS SUBJECT CLASSIFICATION: 39Axx, 58F14, 58F21, 34C05.
KEY WORDS & PHRASES: logistic delay map, bifurcation, non-linear difference equation, perioddoubling.

Report AM-R8402
Centre for Mathematics and Computer Science
P.O. Box 4079, 1009 AB Amsterdam, The Netherlands

1. Introduction

In this paper we consider some aspects of the logistic difference equation containing a delay term

$$x_{n+1} = ax_n(1 - \tfrac{1}{2}x_n - \tfrac{1}{2}x_{n-1}). \tag{1.1}$$

This equation may be considered as the homotopic mean of the well-known equations

$$x_{n+1} = ax_n(1 - x_n), \tag{1.2}$$

and

$$x_{n+1} = ax_n(1 - x_{n-1}), \tag{1.3}$$

cf. [1] and [2].

The model (1.1) written in the form of an iterative planar map

$$\begin{cases} x' = y, \\ y' = ay(1 - \tfrac{1}{2}x - \tfrac{1}{2}y), \end{cases} \tag{1.4}$$

combines the bifurcation behaviour of both (1.2) and (1.3) and is of considerable interest in itself since it presents a case of strong resonance 1:4. The local bifurcation behaviour has been discussed elsewhere [3] and [4]. The equations (1.1), (1.2) and (1.3) are all members of the homotopic family

$$x_{n+1} = ax_n(1 - (1-b)x_n - bx_{n-1}), \qquad 0 \leqslant b \leqslant 1. \tag{1.5}$$

The corresponding two-parameter map, called M, is

$$\begin{cases} x' = y, \\ y' = ay(1 - bx - (1-b)y). \end{cases} \tag{1.6}$$

Its natural domain is the triangular region T bounded by $x > 0, y > 0$ and $bx + (1-b)y < 1$. Let P_0 be a starting point of a trajectory or orbit formed by the successive iterates $P_n = M^n P_0$ then there are various possibilities. P_n may be bounded forever inside T attracted by a fixed point, a cycle of finite period or by a limit cycle and perhaps by a strange attractor. Another possibility is that P_n escapes from T and disappears into infinity. This report is a first step towards obtaining insight into such phenomena of global bifurcation. In particular we consider the case where the non-trivial fixed point of (1.6) $x = y = 1 - 1/a$ is no longer stable. Further we take either $b = \frac{1}{2}$ or b close to $\frac{1}{2}$. This means that the special map (1.4) is our main object of study and that (1.6) is considered a perturbation of (1.4). However, this is mainly a matter of convenience since most considerations are valid for the general case (1.6).

If we consider the map (1.4) for $a > 3$ from an experimental point of view by making plots like fig. 2.3, 2.5 we observe the following behaviour. For $a = 3.1$ there appears to be an attracting 4-cycle. If a increases to the critical value $a_c = 3.29789$ the point plot shows a set of points scattered along a curve that looks like a part of a strange attractor, at least if the trajectory is started close to the origin, but the dominant feature is still that of an attracting 4-cycle. Plots for a larger value of a show that many, most or all trajectories leave T after a few iterations and disappear into infinity. Still, for a up to a second critical value $a_2 = 3.628$ there exists a locally attracting 4-cycle. At this critical value the 4-cycle bifurcates into a locally attracting 8-cycle which is stable up to $a_3 = 3.667$. This is merely the beginning of a Feigenbaum scenario for which $a_9 = 3.674$, the start of a 512-cycle is just detectable on a HP 85 personal computer. However, the attracting domains of the stable 2^m-cycles seem to shrink at each period-doubling. Still for a value of a close to 4 there appear to be patches of a strange attractor with very small and "strange" attracting domains.

In the following sections we shall study the underlying theory needed for understanding the phenomena sketched above. It is merely a beginning of a theory and much has still to be done. We

hope that others may fill in the missing gaps and may develop a more complete theory. In particular we stress the importance of getting a better understanding of the Feigenbaum scenario as sketched in section 5 and the limiting behaviour of the invariant manifolds discussed in section 3.

2. Invariant manifolds

The planar map

$$\begin{cases} x' = y, \\ y' = ay(1-bx-(1-b)y), \end{cases} \tag{2.1}$$

derived from the delayed logistic difference equation

$$x_{n+1} = ax_n(1-(1-b)x_n - bx_{n-1}) \tag{2.2}$$

has the two fixed points $O(0,0)$ and $F(1-1/a, 1-1/a)$. The origin is stable for $|a|<1$. The multipliers of F follow from

$$\lambda^2 - \lambda(2-a-b+ab) + b(a-1) = 0. \tag{2.3}$$

The stability region is determined by (cf. [4])

$$1 < a < Min\left[\frac{3-2b}{1-2b}, 1 + \frac{1}{b}\right]. \tag{2.4}$$

The natural domain for which (2.1) or (2.2) are good models of population dynamics is determined by $a>1$, $0 \leqslant b \leqslant 1$ and $x, y \in T$ where T is the triangle

$$T: x>0, y>0, bx + (1-b)y < 1. \tag{2.5}$$

The map (2.1) may be considered as a Cremona transformation in the projective plane (cf. [4] section 3). This yields for $b \neq 1$ a fixed point at infinity (0,1,0) in homogeneous coordinates. Near this fixed point the map (2.1) can be approximated by

$$\begin{cases} x' = y, \\ y' = -a(1-b)y^2, \end{cases} \tag{2.6}$$

which shows that this point is always locally attracting.

The map (2.1) has the inverse

$$\begin{cases} x = \frac{1}{b} - \frac{1-b}{b}x' + \frac{y'}{abx'}, \\ y = x'. \end{cases} \tag{2.7}$$

For this inverse map F is still a fixed point but O has become a singularity. However, (2.7) has a different fixed point at infinity $(1-b, -b, 0)$ in homogeneous coordinates. Locally (2.7) can be approximated by

$$\begin{cases} x = -\frac{1-b}{b}x', \\ y = x' \end{cases} \tag{2.8}$$

which shows that this point is attracting for $b < \frac{1}{2}$ and repelling for $b > \frac{1}{2}$. In [3] we have shown that it is slowly attracting for $b = \frac{1}{2}$.

For the remainder of this section we take $a>1$ and $b \neq 1$. Then the origin having multipliers 0 and a is unstable with the x-axis as its stable invariant manifold. In fact all points of this line are mapped

onto the origin by a single iteration step. The x-axis is invariant only for the direct map (2.1). If to the x-axis we add all its preimages we obtain a set of lines which as a set is invariant either in forward and backward direction. This set will be studied in the next section. Here we note only that the preimage of $y = 0$ is the line $bx + (1-b)y = 2$ and that the next preimage is a hyperbole.

For $a > 1$ an unstable manifold is attached to the origin as an analytic curve of the kind

$$x = F(t), \quad y = F(at) \tag{2.9}$$

where $F(z)$ is determined by the functional equation

$$F(a^2 z) = aF(az)(1-(1-b)F(az)-bF(z)). \tag{2.10}$$

It is an old result going back to Poincaré, Fatou and many others, that $F(z)$ is an entire function that can be written in the form

$$F(z) = -\sum_{k=1}^{\infty} c_k(-z)^k \tag{2.11}$$

with $c_1 = 1$.

A formal substitution of this series expansion in the functional equation gives the recurrence relation

$$a^k(a^k-1)c_{k+1} = \sum_{j=1}^{k}(ba^{j-1}+(1-b)a^k)c_j c_{k+1-j} \tag{2.12}$$

from which the coefficients can be obtained one after another. In particular for $b = ½$ we have

$$c_1 = 1, \quad c_2 = \frac{a+1}{2a(a-1)}, \quad c_3 = \frac{2a^2+a+1}{4a^3(a-1)^2}. \tag{2.13}$$

Using a computer it is easy matter to calculate $F(t)$ even for quite large values of t by taking the first few terms of the series expansion of $F(t/a^m)$ for a suitable m — making $|t/a^m| << 1$ — followed by iterating (2.10) m times. In this way we have obtained graphs of the unstable manifold for a number of cases. From

$$\begin{cases} x = t - c_2 t^2 + c_3 t^3 - \cdots \\ y = at - a^2 c_2 t^2 + a^3 c_3 t^3 - \cdots \end{cases} \tag{2.14}$$

we obtain by elimination of t

$$y = ax - (a^2-a)c_2 x^2 + (a^3-a)c_3 x^3 - \cdots . \tag{2.15}$$

This is the beginning of another power series expansion but it is of limited use since its convergence is restricted. At the value of x for which $F'(t) = 0$ it starts to diverge. We see that the curved manifold leaves the origin in a parabolic way. Explicitly

$$y = ax - (b + (1-b)a)x^2 + 0(x^3). \tag{2.16}$$

What happens if a is increased from $a = 1$ onwards will be discussed as a description of a set of illustrations for the case $b = ½$. In all of them we have used the scale -0.2, 1.4, -0.2, 1.4 unless stated otherwise.

Fig. 2.1, 2.2 $a = 2.9$

For $7 - \sqrt{32} < a < 3$ the fixed point $F(1-1/a, 1-1/a)$ is a stable focus. Shown is an orbit starting close to O. Successive points converge to F along four branches of a spiral. The next picture shows the curved invariant manifold starting in O and ending in F after an infinite number of turns. All points of the previous plot are on the unstable manifold. If (2.9) is replaced by

$$x = F(a^t), \quad y = F(a^{t+1})$$

the restriction of the planar map to the unstable manifold is merely the shift map.

Fig. 2.3, 2.4 $a = 3.1$
The fixed point F has become unstable. Instead we have a stable 4-cycle formed by 0.9467, 0.5068, 0.4293, 0.7079 and also an unstable 4-cycle formed by 0.8820, 0.6452, 0.4709, 0.6452. The point plot fig. 2.3 shows a single orbit with its starting-point chosen close to the origin. It looks as if four separate orbits are spiralling towards the secondary fixed points. This would really be the case for the iterated map M^4. Fig. 2.4 shows the corresponding unstable manifold of the origin, topologically a halfline on which M is a shift map. This curve approaches the 4-cycle apparently in a most complicated way, at least when seen in a two-dimensional plane.

Fig. 2.5, 2.6 $a = 3.29789$.
For this critical value the unstable manifold of O becomes tangent at the stable manifold $y = 0$ thus developing homoclinic tangency. In terms of the entire function $F(t)$ we have a double zero for some value $t = t_0$ and an infinite number of subsequent double zeros at all multiples $a^k t_0$, $k = 1,2,3....$ This means that the invariant curve has an infinity of branches with cusps at the origin. The successive loops come ever closer to the four members of the attracting 4-cycle in a rhythmic four-beat pattern.
It is instructive to watch a plotter making pictures like fig. 2.6 since this adds a sense of time, an aspect what is missing in those illustrations. If the parameter t of the invariant curve written in the form $x = F(a^t)$, $y = F(a^{t+1})$ is interpreted as time we have roughly a constant speed. However, on loops of higher order the speed can be very high whereas most time is spent in the vicinity of the members of the 4-cycle. Asymptotically jumps are made from one periodic point to the other. At each jump a highly complicated loop is traversed with an infinite speed, an effect escaping observation in actual experiments.

Fig.2.7 $a = 3.675$
For $a > 3.29789$ the invariant curve intersects the stable manifold $y = 0$. Accordingly we have an infinity of loops inside the fundamental triangle T and outside. The outer loops are all in the sector $x < 0, y < 0$. They appear to be attracted by the fixed point at infinity. In order to get a reasonable picture we have plotted $x/(3-x-y), y/(3-x-y)$ on the scale -½, 1½, -1½, 2½. This brings the infinite fixed point in the position 0, -1. We note that $a = 3.675$ is just beyond the Feigenbaum limit of the period-doubling sequence.

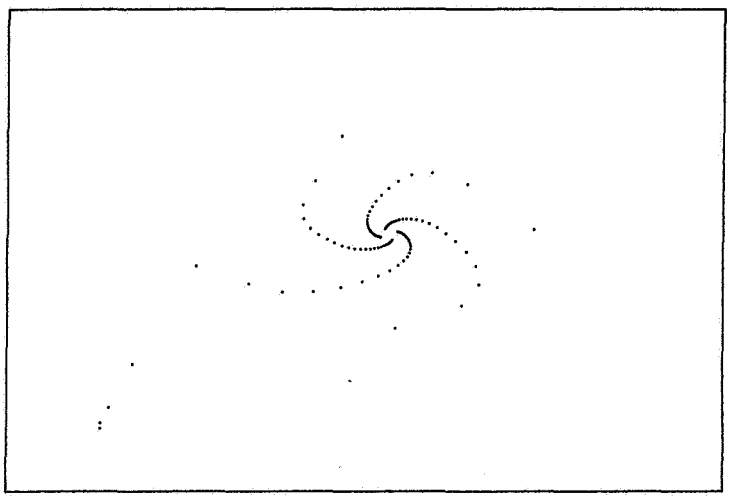

Fig. 2.1

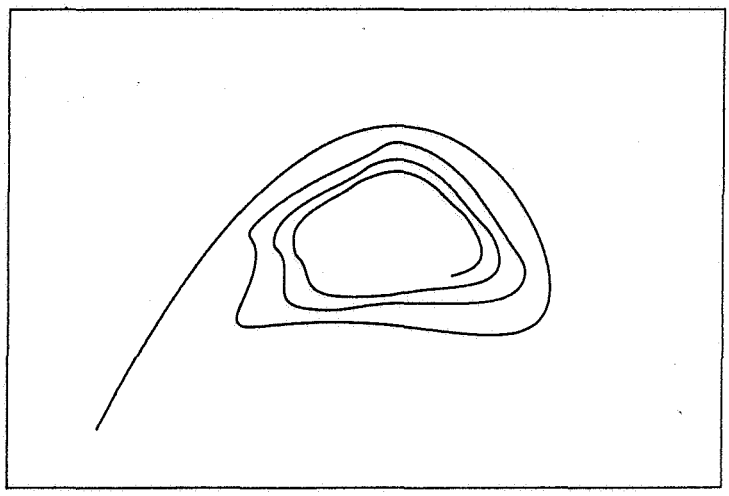

Fig. 2.2

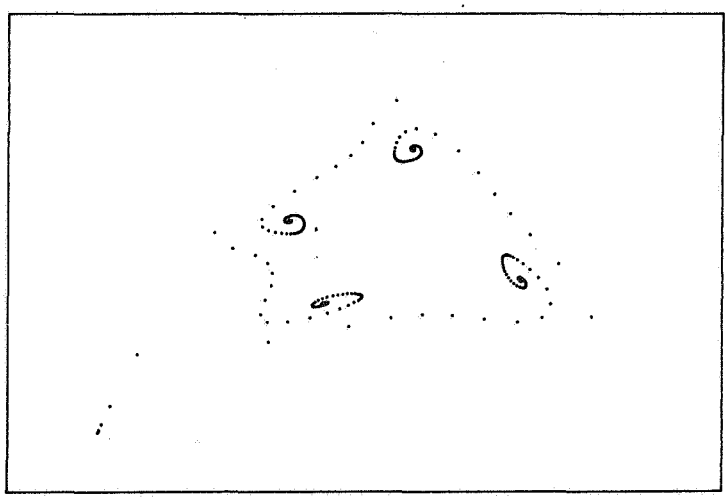

Fig. 2.3

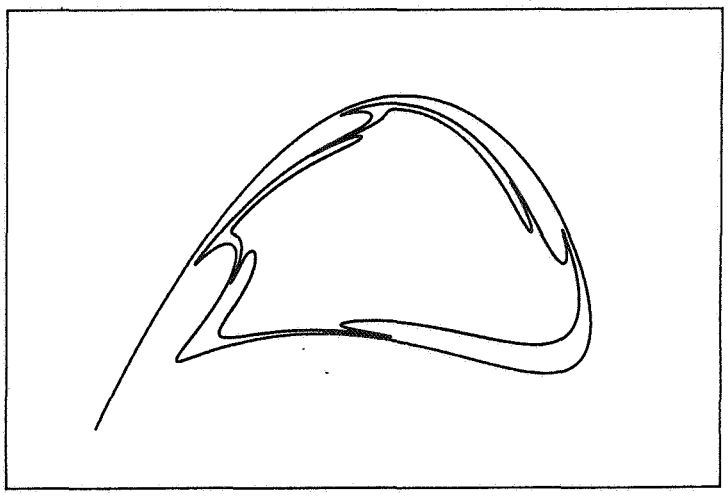

Fig. 2.4

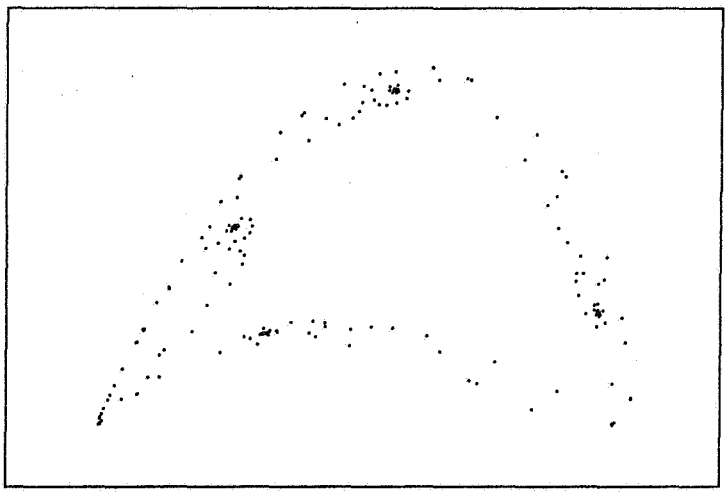

Fig. 2.5

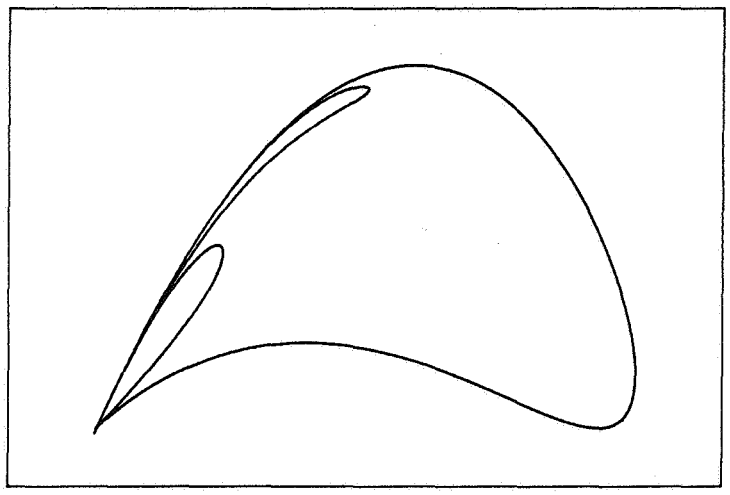

Fig. 2.6

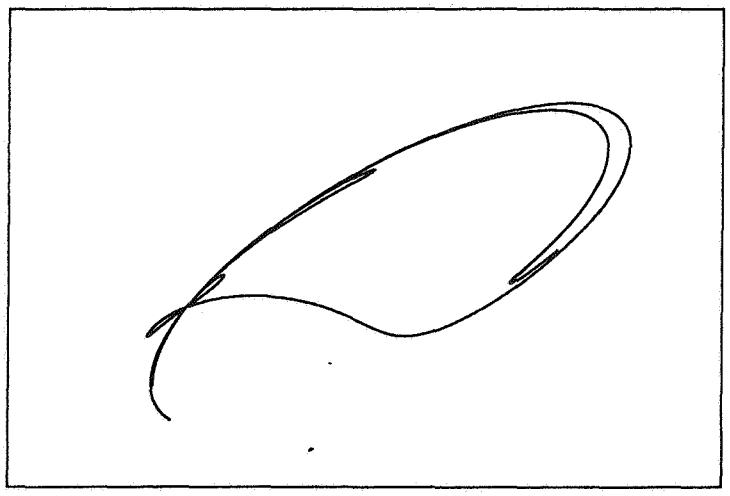

Fig. 2.7

3. Secondary invariant manifolds

For $b = ½$ the map (2.1) has always an unstable 4-cycle consisting of saddle points from which secondary invariant manifolds may emanate. Their form can be determined in very much the same way as in the previous section.

Starting from the difference equation

$$x_{n+1} = ax_n(1 - ½x_n - ½x_{n-1}), \quad a > 3, \tag{3.1}$$

it is easily seen that an unstable 4-cycle is formed by the values

$$x_0 = \sigma_1,\ x_1 = \frac{2}{a},\ x_2 = \sigma_2,\ x_3 = \frac{2}{a}, \tag{3.2}$$

with

$$\begin{cases} a\sigma_1 = a - 1 + \sqrt{(a+1)(a-3)}, \\ a\sigma_2 = a - 1 - \sqrt{(a+1)(a-3)}. \end{cases} \tag{3.3}$$

For the corresponding planar map

$$x' = y, \quad y' = \phi(x, y) \tag{3.4}$$

where

$$\phi(x, y) = ax(1 - ½x - ½y) \tag{3.5}$$

this means a 4-cycle of the following points

$$P_0(\sigma_1, 2/a) \to P_1(2/a, \sigma_2) \to P_2(\sigma_2, 2/a) \to P_3(2/a, \sigma_1).$$

If J_k is the Jacobian

$$\begin{bmatrix} 0 & 1 \\ \phi_x & \phi_y \end{bmatrix}$$

taken at the cyclic point P_k the local matrix at P_0 is given by $J_3J_2J_1J_0$. If λ_1 and λ_2 are its eigenvalues a simple calculation shows that $\lambda_1\lambda_2 = \prod_{k=1}^{4} (\frac{\partial \phi}{\partial x})_k = 1$. A slightly more complicated calculation shows that

$$\lambda_1 + \lambda_2 = (a+1)(a-3)^2 + 2$$

so that the eigenvalue equation can be written in the form

$$(\lambda - 1)^2 = (a+1)(a-3)^2\lambda. \tag{3.6}$$

Example

For $a = 3.5$ we have the 4-cycle

$$(\frac{8}{7}, \frac{4}{7}) \to (\frac{4}{7}, \frac{2}{7}) \to (\frac{2}{7}, \frac{4}{7}) \to (\frac{4}{7}, \frac{8}{7})$$

with

$$\lambda_1 = (25 + 3\sqrt{41})/16 = 2.7631, \quad \lambda_2 = (25 - 3\sqrt{41})/16 = 0.3619.$$

The stable 4-cycle in this case is

$$1.2337,\ 0.3063,\ 0.2466,\ 0.6244$$

rather close to the unstable cycle

1.1429, 0.5714, 0.2857, 0.5714.

In a similar way as in the previous section the unstable manifold at $P_k(x_k, x_{k+1})$ can be described by

$$x = F_k(t), \quad y = F_{k+1}(t) \tag{3.7}$$

where the F_k are entire analytic functions satisfying the equations

$$\begin{cases} F_2(t) = \phi(F_0(t), F_1(t)), \\ F_3(t) = \phi(F_1(t), F_2(t)), \\ F_0(\lambda t) = \phi(F_2(t), F_3(t)), \\ F_1(\lambda t) = \phi(F_3(t), F_0(\lambda t)), \end{cases} \tag{3.8}$$

where λ is the largest eigenvalue of (3.6) and where

$$F_k(0) = x_k. \tag{3.9}$$

The actual calculation of the coefficients, of these functions is straightforward. Writing

$$F_k(t) = x_k + p_k t + q_k t^2 + \ldots, \quad k = 0,1,2,3,$$

we may substitute these series expansions into (3.8). By equating equal powers of t we obtain equations from which the coefficients can be determined successively. At the first step we obtain a homogeneous set of four linear equations which can be solved if λ satisfies the eigenvalue equation. Taking $p_0 = 1$ the coefficients p_1, p_2, p_3 can be calculated. At each subequent step four higher coefficients can be determined by solving an inhomogeneous set of four linear equations. Actually when working on a computer it is sufficient to determine only the first few coefficients, say up to quadratic terms. Then the expansions can be used when t is small. For large values of t we may use the iteration scheme (3.8) a number of times in order to reduce the argument by as many powers of λ as is needed.

In this way we have worked out the case $a = 3.5$ in fig.3.1. The scale is -0.2, 1.4, -0.2, 1.4. The picture may speak for itself. Contrary to what one might believe the invariant curves are not simple arcs or spirals connecting the unstable cyclic point to its stable companion. They have the appearance of little strange attractors with an infinity of folds.

In fig.3.2 a point plot is given for the case $a = 3.678$ using the scale -0.2, 1.4, -0.2, 1.4. It is difficult in this case to find a trajectory which does not escape into infinity. However, there appear to be four local attracting regions. The previous plot suggests that their topological structure might be very complicated.

In fig.3.3 a blow-up is given of the area 0.58, 0.62, 1.28, 1.32 at one of these patches. The plot shows the usual pattern of a strange attractor.

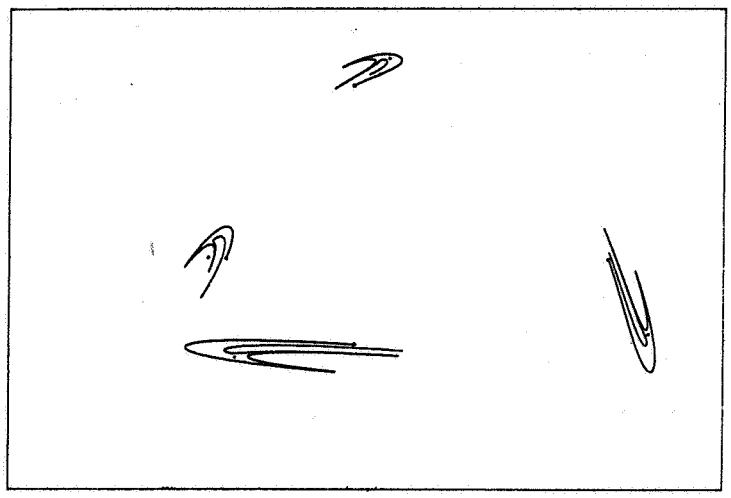

Fig. 3.1 Secondary unstable manifolds for a = 3.5

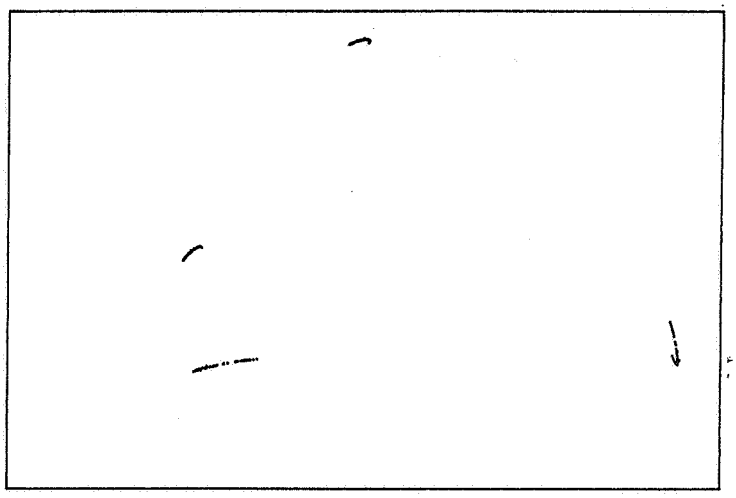

Fig. 3.2

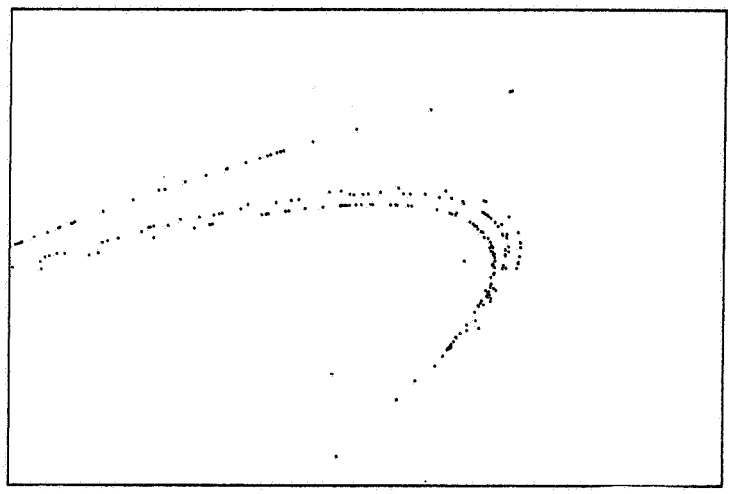

Fig. 3.3

4. Escape regions

Our main interest is the behaviour of the mapping M

$$\begin{cases} x' = y, \\ y' = ay(1 - \tfrac{1}{2}x - \tfrac{1}{2}y), \quad a > 1, \end{cases} \tag{4.1}$$

for points of the basic triangular region

$$T: x > 0, y > 0, x + y < 2.$$

The global mapping properties of M can be read off from diagrams such as given in fig. 4.1 and fig. 4.2 for the special case $a = 3.5$. The object plane is partitioned in twelve parts separated by the lines

$$x = 0, x = 2, y = 0, y = 2, x + y = 2$$

and numbered from 1 to 12. Fig. 4.2 shows the corresponding images according to the following list

$x = 0$	$y = ax(1 - \tfrac{1}{2}x)$
$x = 2$	$y = -\tfrac{1}{2}ax^2$
$y = 0$	$x = y = 0$
$y = 2$	$x = 2$
$x + y = 2$	$y = 0.$

For an orbit starting in $\bar{T}$ there are the following three possibilities

i. After a finite number of steps the orbit ends at the origin.

ii. The orbit stays in T forever.

iii. The orbit eventually escapes into infinity.

The set of all starting points $P(x,y)$ for which the *nth* image P_n coincides with the origin for the first time will be denoted by C_n. A simple observation shows that

$$C_1 \text{ is the line } y = 0$$

$$C_2 \text{ is the line } x + y = 2$$

$$C_3 \text{ is the hyperbole}$$

$$x = \frac{(2-y)(ay-2)}{ay}. \tag{4.2}$$

All further lines are obtained by taking the inverse map: $C_{n+1} = M^{-1}C_n$.

If $P \in T$ is a starting-point of an orbit which escapes into infinity there is an index $n\,(n \geqslant 3)$ such that $M^{n-2}P$ is outside T for the first time. Figures 4.1 and 4.2 show that T is left along the regions marked by $2 \to 3 \to 12$ and that the orbit stays in 12 thereafter. Thus for $P_n = M^n P$ we have $x_n < 0, y_n < 0$. If in (4.1) $x < 0$ and $y < 0$ we see that

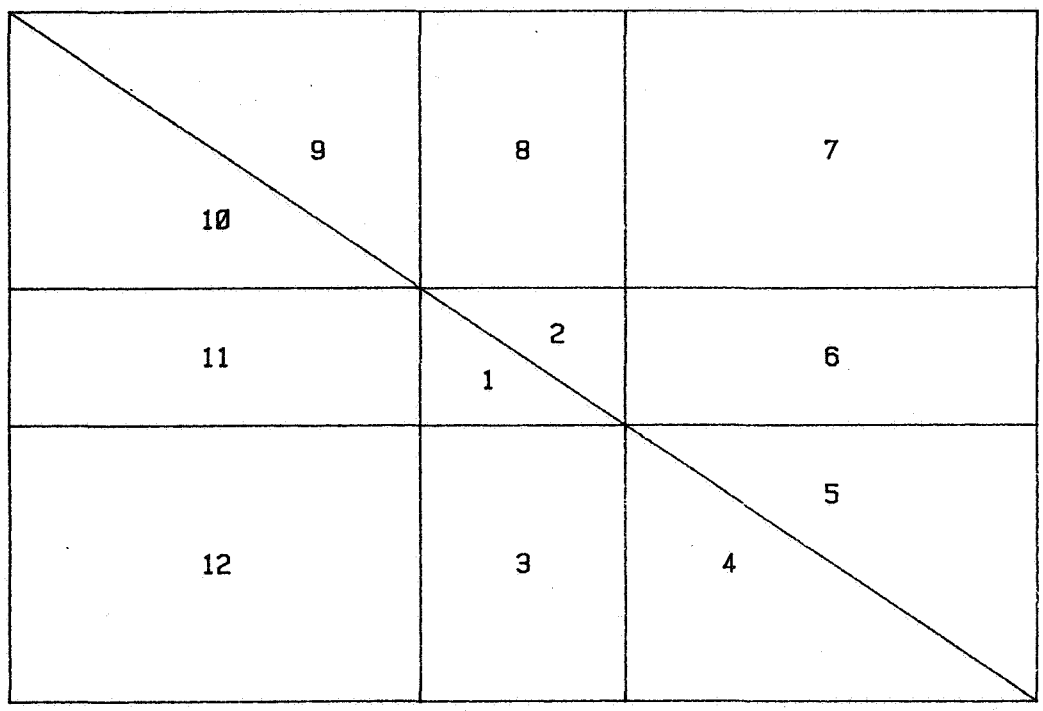

Fig. 4.1 Scale -6, 4, -6, 4 a = 3.5

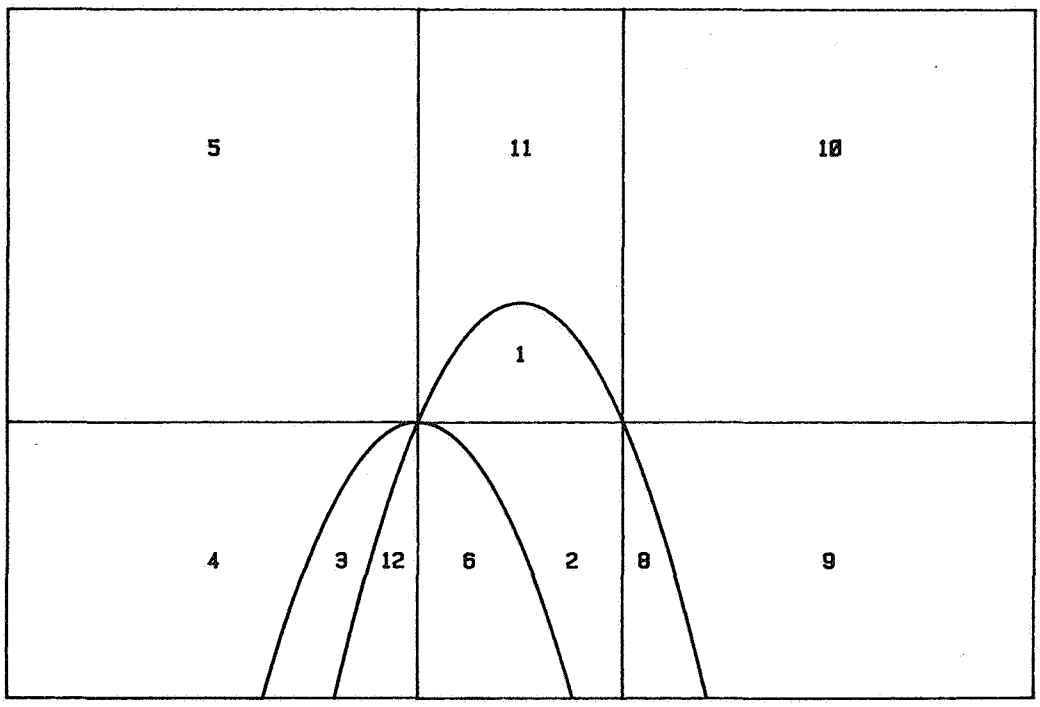

Fig. 4.2

also $y'<0$ and that $|y'|>a|y|$ so that any orbit with a start in 12 escapes into infinity. The set of all starting-points $P \in T$ for which $M^n P$ is in that region for the first time is denoted as E_n, the *nth* escape region. Obviously E_n is bounded by $C_n \cap T$. The first escape region E_3 is bounded by a hyperbolic arc of C_3 and the side $x=0$ as sketched in fig. 4.3.

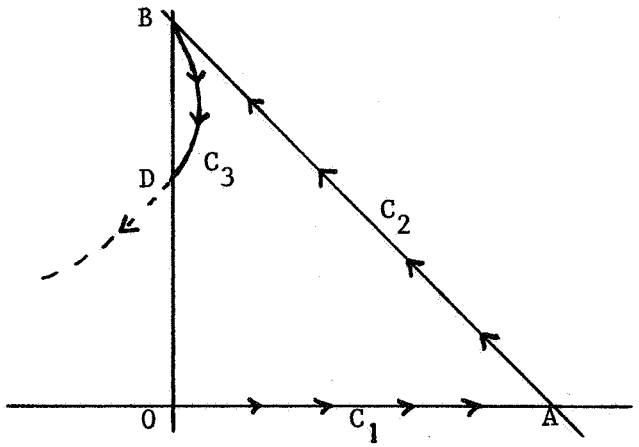

Fig. 4.3

We shall prove that for $1<a<3.20484$ this is the only escape region. This means that all further preimages of $y=0$ are outside T. In order to prove this statement it is sufficient to determine the values of a for which the domain $\bar{T}-E_3$ is mapped into itself. A condition for this is that the parabole $y=ax(1-\frac{1}{2}x)$ and the hyperbolic arc $C_3 \cap T$ do not intersect. Using the computer we find that they become tangent for $a=3.20484$. For larger values of a, however, the situation can be quite complicated with escape regions of arbitrary high index being present in T. In fig. 4.4 we have given a geometrical display of the escape numbers at 19×19 starting-points in a rectangular section

$$0.499<x<0.699, \quad 1.184<y<1.384$$

for $a=3.6265$.
Points with an escape number $n \geqslant 100$ are indicated by H. Those points are good candidates for starting-points of orbits which stay in T forever. The centre is chosen as a stable periodic point with period 4. The resulting diagram suggests a most complicated structure of escape regions. In contrast fig. 4.5 gives with a slightly lower value $a=3.5$ with

$$0.524<x<0.724, \quad 1.134<y<1.334$$

a much - but not essentially - simpler result.

11	11	11	16	12	7	7	7	7	7	12	8	2	2	2	2	2	2	2
11	11	11	11	11	12	7	7	7	7	7	12	8	2	2	2	2	2	2
11	11	17	11	11	11	H	7	7	7	7	7	26	8	2	2	2	2	2
11	16	15	15	15	H	11	11	13	7	7	7	7	45	8	2	2	2	2
11	28	15	32	H	19	15	11	11	12	7	7	7	7	16	8	2	2	2
11	15	19	23	49	79	23	19	16	11	12	7	7	7	7	16	8	2	2
11	24	23	35	23	23	23	23	29	15	11	20	7	7	7	7	22	8	2
11	16	23	23	28	H	H	H	27	39	19	11	16	7	7	7	7	20	8
11	11	19	23	44	31	31	43	H	H	23	71	28	11	7	7	7	7	36
11	11	20	23	H	35	83	H	H	H	H	35	43	25	11	7	7	7	7
11	11	15	H	H	23	35	H	57	27	39	H	H	32	15	11	7	7	7
26	11	15	31	39	19	23	H	43	19	20	66	H	H	37	19	11	13	7
12	11	16	27	23	19	19	H	H	15	16	16	15	19	H	35	31	11	12
13	11	11	23	19	19	19	H	23	29	11	11	11	11	15	27	H	23	11
7	16	11	15	19	78	15	48	31	38	11	11	11	11	11	11	19	H	H
7	21	11	15	29	59	15	23	55	52	11	11	11	49	32	11	11	15	H
7	12	11	16	23	H	15	44	50	15	11	11	20	12	46	12	16	11	11
7	22	11	11	36	23	15	15	H	15	11	11	16	13	6	6	6	17	56
7	7	20	11	22	19	20	15	39	24	11	11	16	13	6	6	6	6	6

Fig. 4.4 Escape numbers for a = 3.6265 in 0.499, 0.699, 1.184, 1.384

11	11	11	11	11	11	60	13	7	7	7	7	H	8	18	2	2	2	2
18	29	28	H	16	11	11	21	21	7	7	7	7	H	8	18	2	2	2
16	15	15	15	15	15	21	11	11	12	7	7	7	7	H	8	33	2	2
16	15	20	19	19	19	15	24	11	11	12	7	7	7	7	H	8	19	2
16	15	19	35	H	H	47	19	15	17	11	16	7	7	7	7	H	8	14
16	15	25	43	H	H	H	H	H	20	20	11	H	7	7	7	7	H	8
H	15	23	H	H	H	H	H	H	H	24	15	11	20	7	7	7	7	H
11	15	23	H	H	H	H	H	H	H	H	47	15	11	H	18	7	7	7
11	15	H	H	H	H	H	H	H	H	H	H	H	24	17	11	22	7	7
11	15	19	H	H	H	H	H	H	H	H	H	H	H	26	16	11	H	7
11	H	19	H	H	H	H	H	H	H	H	H	H	H	H	H	20	11	12
11	16	24	H	H	H	H	H	H	H	H	H	H	H	H	H	80	15	11
11	41	15	H	H	H	H	H	H	H	H	H	H	H	H	H	H	H	15
11	11	15	H	H	H	H	H	H	H	H	27	19	19	19	H	H	H	H
11	11	15	H	H	H	H	H	H	H	H	28	39	15	15	15	19	H	H
33	11	20	H	H	H	H	31	H	H	H	24	15	20	16	16	36	15	31
21	11	34	19	35	31	H	H	32	H	H	23	15	20	11	11	11	11	20
H	11	30	20	H	H	H	H	H	H	H	H	15	32	11	11	11	11	11
30	11	11	15	H	49	H	28	19	23	H	H	28	H	11	11	11	11	11

Fig. 4.5 Escape numbers for a = 3.5 in 0.524, 0.724, 1.134, 1.334

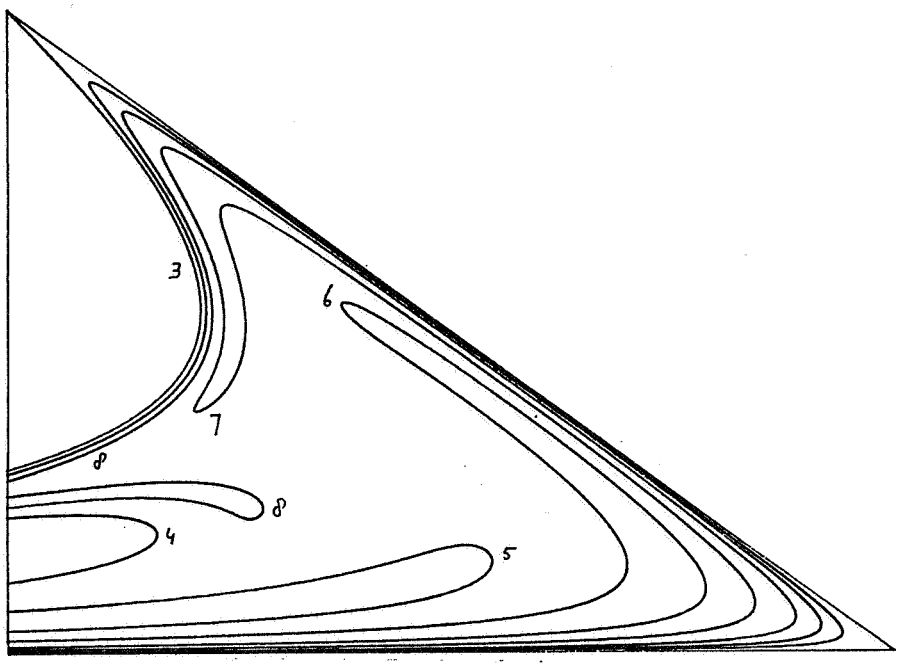

Fig. 4.6 Escape regions for a = 3.5

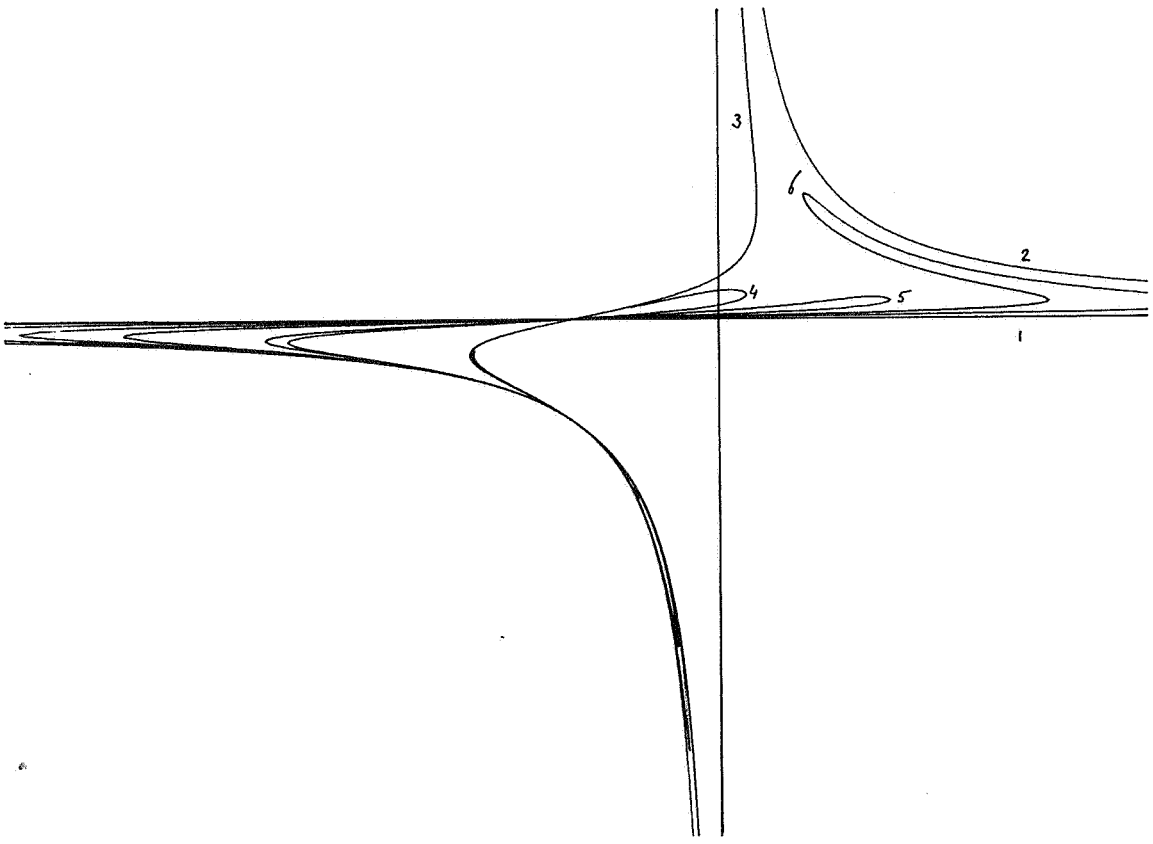

Fig. 4.7 Preimages in the ξ, η-plane for a = 3.5

The preimages C_k of $y=0$ can be parametrised as

$$x=\phi_k(t), \quad y=\phi_{k-1}(t) \tag{4.3}$$

where

$$\phi_0(t)=0,$$
$$\phi_1(t)=t,$$
$$\phi_2(t)=2-t,$$

and generally

$$\phi_{k+1}(t)=2-\phi_k(t)-\frac{2\phi_{k-1}(t)}{a\phi_k(t)}. \tag{4.4}$$

The overall behaviour of $\phi_k(t)$ is characterised by clusters of zeros and asymptotes. Each $\phi_k(t)$ inherits the asymptotes from previous functions and has further asymptotes at the zeros of $\phi_{k-1}(t)$. A typical cluster of zeros is e.g.

$k=3$	$t=1.429$
4	1.3132
5	1.30284
6	1.3027026
7	1.30270218
8	1.302702169

This behaviour can be understood by using a little perturbation analysis. Let $\phi_{k-1}(t)$ have the zero t_{k-1} and let $\phi_k(t)$ has a neighbouring zero t_k then locally

$$\phi_k(t)\approx\frac{c_k(t-t_k)}{t-t_{k-1}}. \tag{4.5}$$

Considering (4.4) for t close to t_k and t_{k+1} we obtain the relations $c_k\approx 2$ and

$$\Delta_{k+1}\approx\frac{2\Delta_k^2}{a\Delta_{k-1}}, \tag{4.6}$$

where

$$\Delta_k=t_{k-1}-t_k. \tag{4.7}$$

This shows that

$$\log\frac{1}{|\Delta_k|}=\tfrac{1}{2}k^2\log\frac{2}{a}+O(k). \tag{4.8}$$

The recursion (4.4) can be used to obtain the first few preimages C_n of $y=0$. In this way in fig. 4.6 the escape regions E_n have been obtained for $a=3.5$ up to $n=8$. It is a matter of interest to have some information on the shape of the escape boundaries C_n outside T. In fig. 4.7 we have plotted the first few C_n in the (ξ,η)-plane where

$$\xi=\frac{1}{2-x}, \quad \eta=\frac{1}{2-y}. \tag{4.9}$$

It is not difficult to show that all points of $x=2$, with the trivial exception $x=2, y=0$, belong to either the extended escape region E_2 or to E_3. This means that for $n\geq 4$ C_n has no points on $x=2$ and $y=2$. Therefore all curves C_n for $n\geq 4$ become closed curves in the ξ,η-plane in the region bounded by C_1, C_2, C_3. Returning to the x,y-plane we see that all preimages of $y=0$ are in the region

$$\begin{cases} \dfrac{(2-y)(ay-2)}{ay} \leqslant x \leqslant 2-y & \text{for } 0 \leqslant y \leqslant 2, \\ 2-y \leqslant x \leqslant \dfrac{(2-y)(2-ay)}{-ay} & \text{for } y \leqslant 0. \end{cases} \tag{4.10}$$

Diagrams like fig. 4.4 and 4.5 give an impression of the complexity of the escape regions of higher order and of the complementary invariant set of orbits that stay in T forever. In order to obtain some more information we consider what happens at the boundary OB of fig. 4.3.
As a increases more and more escape regions enter T along the boundary OB in a tongue-like fashion. We consider a point of OB as the starting-point of an orbit which either stays in T forever or leaves T after m steps. Thus to each point of OB we may associate an escape number m possibly ∞. More precisely we denote by I_m the set of all points $(0,y_0)$ for which $y_m<0$ and $y_k>0$ for $k<m$. Of course I_m is open and consists of a finite number of open intervals. We may state the following important property.

Theorem 4.1

I_m and I_n $(m \neq n)$ cannot have a common boundary point.

Proof Let $P(y_0)$ be a possible boundary point of both I_m and I_n with $m<n$. Consider a small interval $E(y_0-\epsilon<y<y_0+\epsilon)$ and consider its iterate $M^{m+1}E$ which brings P to the origin and $E \cap I_n$ to an ϵ-neighbourhood of the origin still inside T. Close to the origin we have $x' = y$, $y' \approx ay$. If y is sufficiently small then after $n-m$ iterations we are still inside T but this contradicts the assumption of a finite n. □

This theorem shows that there exists a non-empty closed set of starting-points the orbits of which stay forever inside T. For values of a in the interval (3.5,4) this set looks like a Cantor set. In fig. 4.8 we have shown the results of a computer experiment in which for $a = 3.7$ for 200 points of OB the escape number $(1<m \leqslant 50)$ is plotted. The graph pictures a transsection through the various escape regions.

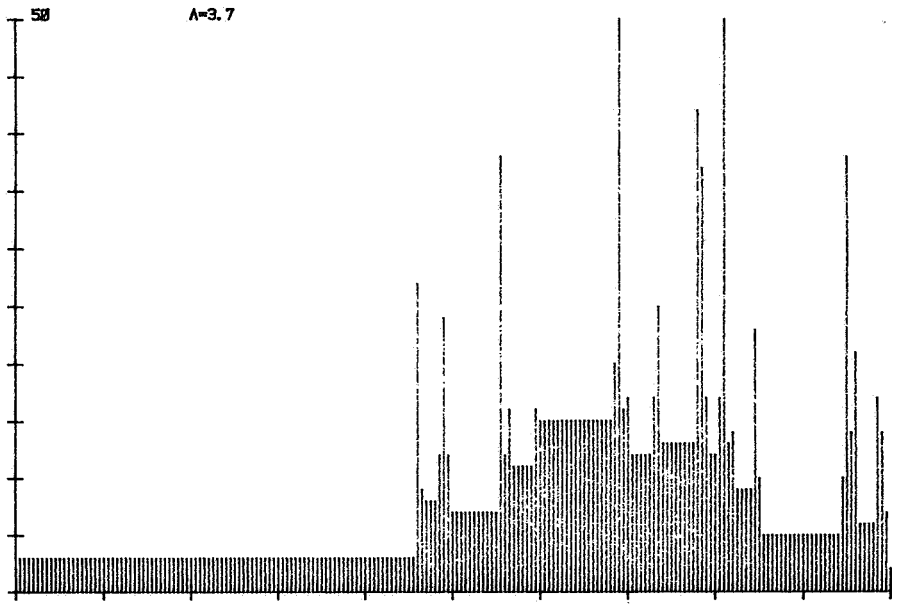

Fig. 4.8 Escape numbers along x = 0, 0 < y < 2 for a = 3.7

5. A Feigenbaum scenario

The two-step iterative sequence

$$x_{n+1} = a x_n (1 - \tfrac{1}{2} x_n - \tfrac{1}{2} x_{n-1}) \tag{5.1}$$

has the non-trivial fixed point $x_f = 1 - 1/a$ which becomes unstable when a passes the critical value 3. In [3] we have considered the corresponding map

$$\begin{cases} x' = y, \\ y' = a y (1 - \tfrac{1}{2} x - \tfrac{1}{2} y), \end{cases} \tag{5.2}$$

and shown the existence of a stable 4-cycle and an unstable 4-cycle bifurcating from $x = y = 1 - 1/a$. The unstable cycle of (5.1) exists for all $a > 3$ as

$$\frac{2}{a}, 1 - \frac{1}{a} + \frac{\sqrt{(a+1)(a-3)}}{a}, \frac{2}{a}, 1 - \frac{1}{a} - \frac{\sqrt{(a+1)(a-3)}}{a}. \tag{5.3}$$

For $a = 3 + \mu$ with μ positive and small the stable cycle can be approximated by

$$x_f(1 + C_1\sqrt{\mu}), x_f(1 + C_2\sqrt{\mu}), x_f(1 - C_1\sqrt{\mu}), x_f(1 - C_2\sqrt{\mu}) \tag{5.4}$$

with

$$C_1 = \sqrt{1 - 1/\sqrt{2}},\ C_2 = \sqrt{1 + 1/\sqrt{2}}. \tag{5.5}$$

As a numerical check we take $\mu = 0.0001$ with the exact values

0.670286, 0.675512, 0.662904, 0.657872

in excellent agreement with (5.4).

The stable cycle stays stable up to the value $a_2 = 3.628$. Next it bifurcates into an 8-cycle which is stable up to $a_3 = 3.667$. This is the beginning of a long sequence, presumably infinite, of pitchfork bifurcations characterised by a multiplier becoming -1. Let a_m be the value at which a 2^m-cycle bifurcates into a 2^{m+1}-cycle then the following table can be constructed

m	a_m	$a_{m+1} - a_m$	
1	3	6.27630	$\times 10^{-1}$
2	3.62762975649	3.89682	$\times 10^{-2}$
3	3.66659796056	5.92358	$\times 10^{-3}$
4	3.67252153677	1.15475	$\times 10^{-3}$
5	3.67367628354	2.46812	$\times 10^{-4}$
6	3.67392309602	5.28993	$\times 10^{-5}$
7	3.67397599537	1.13356	$\times 10^{-5}$
8	3.67398733095	2.42803	$\times 10^{-6}$
9	3.67398975898	5.20025	$\times 10^{-7}$
10	3.67399027900	1.11374	$\times 10^{-7}$
11	3.67399039038	2.38529	$\times 10^{-8}$
12	3.67399041423	5.10857	$\times 10^{-9}$
13	3.67399041934		

Before this table is discussed we shall first describe the numerical procedure by means of which accurate values of a_m can be obtained in a relatively simple way.

Let us assume that the planar map (5.2) denoted as $P' = M(P)$ has the stable 2^m-cycle $S_1, S_2, \ldots, S_{2^m}$ then each member of the cycle is an ordinary fixed point of the iterated map M^{2^m}. Its multipliers λ_1, λ_2 which are the same for all points of the cycle are the eigenvalues of the matrix J

formed as the product of 2^m local matrices of F at the successive cyclic points

$$J = J(S_{2^m})J(S_{2^m-1})...J(S_2)J(S_1). \tag{5.6}$$

The general situation is as follows. If a increases slightly one of the multipliers runs along the real axis from $+1$ to -1 whereas the other multiplier stays close to zero. For $a = a_m$ we have, say, $\lambda_1 = -1$ and $|\lambda_2| << 1$. Writing J as

$$\begin{bmatrix} A & B \\ C & D \end{bmatrix}$$

we define

$$\begin{cases} p = \lambda_1 + \lambda_2 = A + D, \\ q = \lambda_1 \lambda_2 = \det J. \end{cases} \tag{5.7}$$

At the bifurcation point we have

$$p + q + 1 = 0. \tag{5.8}$$

This suggests the following numerical procedure. If for a given value of $a \in (a_{m-1}, a_m)$ we have obtained the cycle $S_1, S_2, ..., S_{2^m}$ we compute the elements of J and determine the value of $p + q + 1$ using (5.7). In principle for each value of a we get such a value thereby obtaining a function $\phi(a)$. Obviously the desired value $a = a_m$ is a zero of this function. This criterion appears to be extremely sensitive. The last stage, the finding of the root of $\phi(a) = 0$, does not give any problems. The only time-consuming part is the determination of a sufficiently accurate cycle $S_1, S_2, ...S_{2^m}$ for a given value a. We have used the following procedure.

Let us assume that a is already sufficiently close to a_m so that $\lambda_1 \approx -1$ and $|\lambda_2| << 1$. We write $\lambda_1 = -1 + \epsilon$. Let P_1 be an approximation of the cyclic point S_1 then after 2^m elementary iterations we arrive at ϕ_1 which is also close to S_1. Another 2^m steps bring us at R_1. In this way we have three successive approximations of S_1. The deviations are locally linear compositions of powers of λ_1 and λ_2. This suggests approximations of the following form

$$\begin{cases} x(P_1) = x(S_1) + \alpha + ... \\ x(\phi_1) = x(S_1) - \alpha(1 - \epsilon) + ... \\ x(R_1) = x(S_1) + \alpha(1 - \epsilon)^2 + ... \end{cases} \tag{5.9}$$

and similarly for the y-values.

From this a much better estimate of $x(S_1)$ is obtained as

$$\frac{1}{4}(x(P_1) + 2x(Q_1) + x(R_1)), \tag{5.10}$$

etcetera.

The next problem is the determination of the elements of the matrix J. We have of course

$$q = \prod_{k=1}^{2^m} \det J(S_k) = \prod_{k=1}^{2^m} (a y(S_k)/2) \tag{5.11}$$

but p cannot be determined in a similar way. However, the elements of J can be determined recursively by using

$$\begin{bmatrix} A_{k+1} & B_{k+1} \\ C_{k+1} & D_{k+1} \end{bmatrix} = \begin{bmatrix} 0 & 1 \\ -\frac{1}{2}ay_k & a(1 - \frac{1}{2}x_k - y_k) \end{bmatrix} \begin{bmatrix} A_k & B_k \\ C_k & D_k \end{bmatrix}. \tag{5.12}$$

which gives the iterative scheme

$$\begin{cases} A_{k+1} = C_k, \\ B_{k+1} = D_k, \\ C_{k+1} = -\tfrac{1}{2}ay_k A_k + a(1-\tfrac{1}{2}x_k - y_k)C_k, \\ D_{k+1} = -\tfrac{1}{2}ay_k B_k + a(1-\tfrac{1}{2}x_k - y_k)D_k. \end{cases} \tag{5.13}$$

If this scheme is used for $k=1$ up to $k = 2^m - 1$ with the start

$$A_1 = 0,\ B_1 = 1,\ C_1 = -\tfrac{1}{2}ay_1,\ D_1 = a(1-\tfrac{1}{2}x_1 - y_1) \tag{5.14}$$

the elements of J can be determined. Since q can be computed either by (5.11) or as $AD - BC$ we have a simple numerical check.

Inspection of the table suggests a Feigenbaum sequence of the kind

$$a_{m+1} - a_m = C\delta^{-m} + \ldots \tag{5.15}$$

where $\delta = 4.6692$ is Feigenbaum's constant. In order to test this hypothesis the following table is made

m	$(a_{m+1} - a_m)/(a_{m+2} - a_{m+1})$
1	16.10620
2	6.57849
3	5.12976
4	4.67864
5	4.66570
6	4.66667
7	4.66863
8	4.66907
9	4.66917
10	4.66920
11	4.66920

The convergence to δ appears to be rather slow in contrast to the very good convergence observed in a similar table for the well-known iterative map $x' = ax(1-x)$.

References

[1] J.R. Pounders and Th.D. Rogers (1982). *The geometry of chaos: Dynamics of a nonlinear second-order difference equation.* Bull. Math. Biology, 42, 551-597.

[2] D.G. Aronson et al (1982). *Bifurcation from an invariant circle for two-parameter families of maps of the plane. A computer assisted study.* Comm. Math. Phys. 3, 303-354.

[3] H.A. Lauwerier (1983). *Bifurcation of a map at resonance 1:4.* Report TW 244, Mathematisch Centrum, Amsterdam.

[4] H.A. Lauwerier (1983). *Local bifurcation of a logistic delay map.* Report TW 245, Mathematisch Centrum Amsterdam.

ONTVANGEN 2 2 MAART 1984